



Lawrence Berkeley Laboratory

UNIVERSITY OF CALIFORNIA

Materials & Molecular Research Division

Presented at the International Cryogenic Materials Conference,
Madison, WI, August 21-24, 1979; and to be published in
Advances in Cryogenic Engineering

A STUDY OF FERRITIC WELD DEPOSITS IN Fe-9Ni STEEL

K. W. Mahin and J. W. Morris, Jr.

August 1979

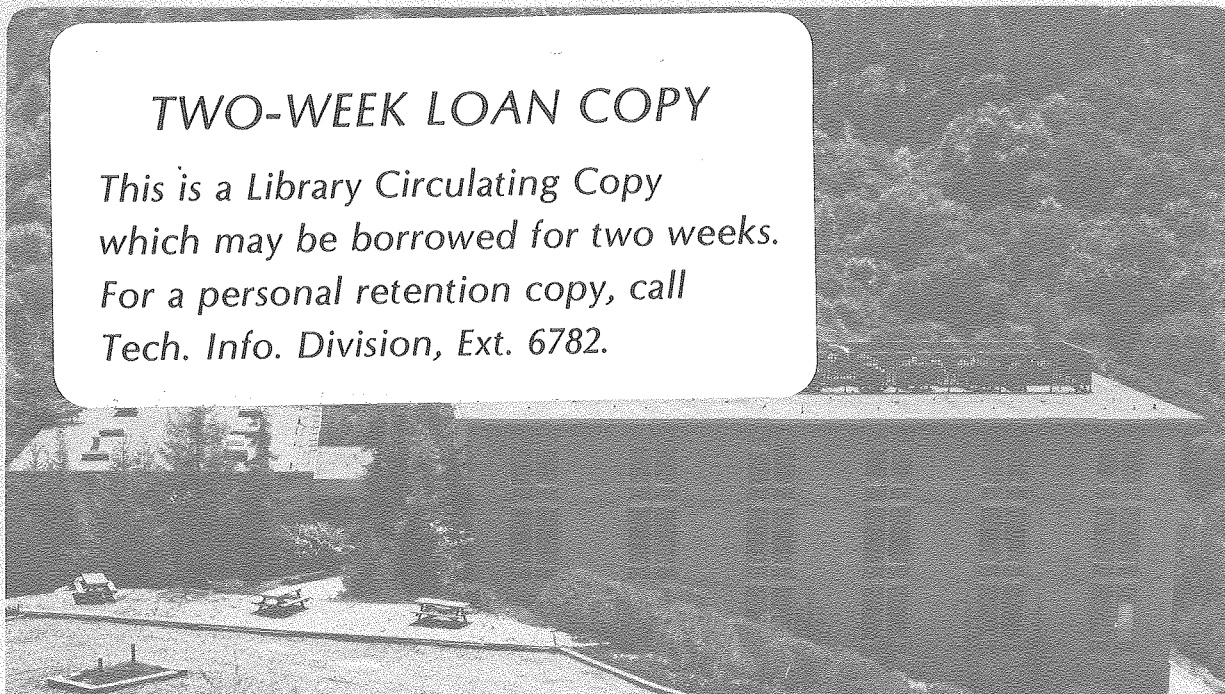
RECEIVED
LAWRENCE
BERKELEY LABORATORY

FEB 25 1980

LIBRARY AND
DOCUMENTS SECTION

TWO-WEEK LOAN COPY

*This is a Library Circulating Copy
which may be borrowed for two weeks.
For a personal retention copy, call
Tech. Info. Division, Ext. 6782.*



LBL-10130 c.2

DISCLAIMER

This document was prepared as an account of work sponsored by the United States Government. While this document is believed to contain correct information, neither the United States Government nor any agency thereof, nor the Regents of the University of California, nor any of their employees, makes any warranty, express or implied, or assumes any legal responsibility for the accuracy, completeness, or usefulness of any information, apparatus, product, or process disclosed, or represents that its use would not infringe privately owned rights. Reference herein to any specific commercial product, process, or service by its trade name, trademark, manufacturer, or otherwise, does not necessarily constitute or imply its endorsement, recommendation, or favoring by the United States Government or any agency thereof, or the Regents of the University of California. The views and opinions of authors expressed herein do not necessarily state or reflect those of the United States Government or any agency thereof or the Regents of the University of California.

A STUDY OF FERRITIC WELD DEPOSITS IN Fe-9Ni STEEL

By K. W. Mahin and J. W. Morris, Jr.

Department of Materials Science and Mineral Engineering
Materials and Molecular Research Division
Lawrence Berkeley Laboratory
University of California, Berkeley

INTRODUCTION

In 1977, research was initiated at the Lawrence Berkeley Laboratory to study the factors influencing low temperature toughness levels in ferritic gas metal arc (G.M.A.W.) weldments of 9% Ni steel. Commercial plates of this steel have yield and tensile strengths on the order of 136 ksi (938 MPa) and 170 ksi (1172 MPa) respectively (Table 1). The gas metal arc (G.M.A.W.) consumables currently used for fabrication of 9% Ni steel low temperature containment vessels are of the high-nickel-chrome or modified austenitic types¹⁻⁵, having yield strengths of 60-80 ksi (414-552 MPa) and tensile strengths of 90-120 ksi (621-828 MPa). From an economic, as well as design standpoint, a more acceptable filler metal would be a matching low-nickel ferritic weld wire. However, attempts made to date to produce a commercially acceptable ferritic gas metal arc weld wire have been unsuccessful⁶. The approach taken in this work has been to evaluate different ferritic gas shielded arc filler wires in terms of their chemistry, microstructure, toughness properties and fracture modes.

EXPERIMENTAL PROCEDURES

A. Materials and Welding Procedures

The current studies were carried out using Armco Steel's 5/8 in. (16 mm) thick commercial A553-Grade A quenched and tempered 9% Ni steel for the weldment base plate and four different low-nickel ferritic wire compositions as the filler metals. Table 1 presents the chemical and mechanical properties of the base plate; Table 2 indicates the wire chemistries of the four ferritic consumables. The first three compositions in Table 2 were made into wire by hand-swaging 5 lb. (2.3 kg.) induction furnace heats into 20 ft. (6 m.) lengths of 1/16 in. (1.6 mm) wire followed by extensive surface cleaning. The last wire, produced from two 25 lb. (11 kg.) vacuum cast ingots, was commercially drawn into wire by U. S. Welding in California. All test plates were welded using a modified Miller Spoolmatic II gas metal arc electrode gun in either the semiautomatic or automated modes, with a shielding gas of 75% Helium - 25% Argon. The heat input in all cases was restricted to below $\frac{(1.2 \text{ kJ/mm})}{30 \text{ kJ/in.}}$, with the average being $\frac{(0.9 \text{ kJ/mm})}{24 \text{ kJ/in.}}$. All plates were strapped to copper chill bars and fully restrained during welding, with the maximum interpass temperature maintained below 60°C (140°F).

The weldments made with the first three wires in Table 2 were fabricated using a single-V, 70° included angle design; the last weldment was made with both a double-bevel and single-bevel, 45° included angle preparation, in order to provide more controlled testing of the weldment zones. Grinding of the weld bead was done only in cases where visible defects were in evidence. All plates were evaluated before mechanical testing using X-Ray radiography and ultrasonic

techniques to detect defects.

B. Methods of Analysis

Mechanical testing was done at -196°C using Charpy-V-notch specimens and three-point bend specimens for most of the evaluation. Fracture surfaces were studied using an AMR 1000 scanning electron microscope with attached EDX unit for chemical analyses. A PHI 590A scanning Auger microprobe with a minimum spot size of $.3\ \mu\text{m}$ was used to analyze the surface chemistry of the brittle regions. Determination of the amount of retained austenite in the weldment was performed using a Mössbauer backscattering spectrometer which measured the atomic fraction of austenite to within $\pm.5\%$. Since the Mössbauer effect is a nuclear resonance phenomenon and not a diffraction effect, it is suitable for welds which have a high degree of preferred crystallographic orientation.

RESULTS AND DISCUSSION

A. Toughness Properties

The welds made with the four ferritic wire compositions listed in Table 2 were evaluated for notch sensitivity at -196°C using Charpy-V-notch specimens. The results of these tests are shown in Fig. 1. Wire composition 778-5, which was based on the gas tungsten arc ("TIG") wire chemistry published by I. Watanabe in 1977⁷, produced a ferritic weldment with an impact toughness of 120 ft-lb. (163J) at -196°C in the defect-free regions. However, the level of defects in the weld was high, 80% rejectable porosity, as expected from the lack of sufficient deoxidizers in the wire chemistry. Unlike the weldments fabricated with the other wires, the 778-5 weld was made using a special low sulfur (.002 wt.%), low phosphorus (.003 wt.%) base plate, in order to

better correlate the gas metal arc weldment results with those obtained by Watanabe using the gas tungsten arc (G.T.A.W.) process. The chemistry of wire 778-6 was based on the optimum composition reported in F. H. Lang's 1975 patent⁸. The base plate for these test weldments was the commercial A553 plate described in Table 1. Although there was an absence of detectable defects in this weld, the toughness level in the weld deposit was only 20 ft-lb. (27J) energy at -196°C.

Wires 786-1 and LCMM-1 were proposed as modifications of these previous compositions. Tests to date on the LCMM-1 weld deposits have resulted in properties ranging from 15 to 25 ft-lb. (20-34J) impact energy at -196°C as indicated in Figure 1. The cause of this embrittlement can be attributed most obviously to the presence of lack of fusion defects not detected in the nondestructive evaluation and to the unfavorable aligned growth of the dendrites parallel to the thickness direction of the weld. Wire 786-1, on the other hand, produced sound welds with good impact and fracture toughness properties in the weld metal of 40 ft-lb. (54J) and 125 ksi- $\sqrt{\text{in.}}$ (137 MPa- $\sqrt{\text{in.}}$) respectively at liquid nitrogen temperatures, (Fig. 1).

B. Analysis of Fracture Modes

In each of the weldments studied, the weld metal microstructure was characterized by regions of large columnar grains separated by grain-refined areas. The extent of grain refinement varied in each case but the 786-1 and 778-5 weldments developed the maximum degree of refinement. However, grains as large as 200 μm in size were in evidence in the 778-5 weldment, but displayed signs of having undergone recrystallization at the grain boundaries.

Although the toughness behavior of 778-5 is of some interest, the main thrust of this report is focused on the characteristics of the ferritic low-nickel deposits produced by wire compositions 786-1 and LCMM-1. In the case of the 786-1 weld deposit extensive grain refinement was found to have occurred in the center of the weld, with excessive columnar grain growth in evidence only in the final face and root passes. The grain refined regions of the LCMM-1 weld deposits were restricted to thin layers between weld passes, with aligned columnar grains of about 300 μm - 400 μm in size in evidence throughout the weld metal.

The results obtained from a Mössbauer scan of the relative atomic fractions of austenite and martensite in the LCMM-1 weldment are indicated in Figure 2a. The weld metal retained less than .5% of the austenite phase as compared to the base metal levels of 5% to 7%. Similar results were obtained for the 786-1 weld deposit. Stress-relieving of the LCMM-1 samples at 1050°F (566°C) for 2 hours was performed in an attempt to improve toughness. Although the level of retained austenite increased to between 1% and 1.5%, as indicated in Fig. 2b, toughness levels were only slightly improved: 27 ft-lb. (37J) at -196°C. However, this could have been the result of defects rather than phases in the weld deposit. In order to determine the approximate level of retained austenite that would be present in the deposit in the absence of high restraint stresses, a 1/2 in. (13 mm) diameter ingot with a chemistry approximating that of the weld deposit was quenched after casting at rates simulating those encountered during welding. The casting had 1.5% retained austenite as shown in Fig. 2b. The

characteristics of the martensite formed from the transformed austenite in the weld metal are still to be evaluated and its relation to the toughness of the deposit determined.

Optical and scanning electron microscope (SEM) micrographs of the low toughness weld deposit fractures of LCMM-1 are presented in Figs. 3(a)-(f). In regions where the cleavage path was not parallel to the dendrite axis, Figs. 3(a)-(c), fracture was transgranular, and cleavage steps associated with transitions in martensite packets, as indicated in Fig. 3(c). When the fracture path was aligned parallel to the dendrite axis, Figs. 3(d)-(f), a distorted type of quasi-cleavage fracture occurred. At higher magnifications (Figs. 3e-3f), it is apparent that fracture occurred in regions adjacent to the interdendritic regions with occasional deviations through the dendrite or boundary regions. There was no evidence to suggest that the presence of martensite packets influenced the path of this fracture to any large extent. Dendrite segregation patterns were also in evidence on the fracture surface (Fig. 3(f)).

The results of an analysis of the fracture mode of the higher toughness 786-1 weld deposit are presented in Fig. 4(a)-(f). The microvoid coalescence region, detailed in Figs. 4(a)-4(c), was associated with a grain-refinement of the deposit, as indicated in Fig. 4a. The "fiber-like" dimpled regions on the fracture surface, pointed out in Fig. 4c, were the result of fracture along the interdendritic boundaries, as was shown by comparison with Fig. 4(b). This differed from the distorted quasi-cleavage type of fracture associated with these boundaries in the LCMM-1 weld deposit. In coarser grained regions,

the cleavage was again transgranular and associated itself preferentially with the martensite packets, Figs. 4d-4f.

In order to determine whether the lower toughness of the LCMM-1-2 weldment was the result of chemical segregation, a series of scanning Auger microprobe studies were performed on both the polished and the fracture surfaces. Fig. 5 shows the results of surface chemistry scans of an ion-milled region of the polished surface. Three regions were evaluated by point analysis using a submicron spot size. Region A, located inside the dendrite, had the highest concentration of nickel relative to the iron peak. This puzzling result was also found by EDX measurements and may be the result of a multiple element interaction. Furthermore, the Fe/Ni ratios calculated for the interdendritic and high angle boundary regions indicated that nickel was depleted in these areas. Submicron sized molybdenum and possibly also titanium carbides were present in all regions. Sulfur was detected in both the dendrite matrix and the interdendritic regions, while phosphorus was present only at the high angle boundary. The sulfur in the matrix is probably associated with manganese, whose peak overlaps the iron peak.

Scans of an LCMM-1 Charpy fracture surface are presented in Fig. 6. Point 1 of this analysis had an Fe/Ni ratio of 6.9 with small amounts of sulfur, molybdenum and titanium present. Comparison of this scan with that obtained in Fig. 5 for the dendrite matrix seems to indicate that fracture occurred in the dendrite matrix in a manner similar to that shown in Figs. 3(e)-(f). On the other hand, the Fe/Ni ratio for point 2 is 8.0, which would appear to indicate that fracture in this region was associated with the dendrite boundary. The highest nickel

concentration occurred at point 3, with an Fe/Ni ratio of 6.2. The absence of S, P, Mo, or Ti in the scan of this area would appear to indicate that the fracture was located in the center of a dendrite.

The particular features of these scans, when evaluated in light of the solidification features of the weld deposit, seem to indicate that the type of quasi-cleavage fracture shown in Figs. 3 e-f is not due to a chemical segregation of embrittling elements. It may be that a second phase has formed in these regions. However, these conclusions are tentative and require further investigation.

CONCLUSION

Four ferritic gas metal arc weld wire compositions have been evaluated in this report in terms of their toughness properties and microstructural features. Mössbauer scans of the weld deposits indicate an absence of retained austenite, although rapidly cooled castings of a chemistry similar to that of the weld deposits, as well as air-cooled stress-relieved weldment samples, contain 1.5% retained austenite. Scanning Auger studies of the surface chemistry of the polished microstructure and the fracture surface have revealed interesting correlations, which will be investigated further.

ACKNOWLEDGMENT

The preparation of this review and portions of the research cited here were supported by the Office of Materials Science, Division of Basic Energy Sciences, U. S. Department of Energy under contract W-7405-ENG-48.

REFERENCES

1. N. Bailey: Met. Constr. and Brit. Weld. J., 2, (10), 419-421, (October 1970).
2. R. H. Tharby: Weld. and Met. Fab., 41, (2), 51-61, (February 1973).
3. R. A. Daemen: Proc. of Int'l Conf. on Welding Low Temp. Containment Plant, Welding Institute, London, England, Paper 2, (November 1973), p. 10.
4. W. E. Morgan and P. L. Norman: Proc. of Int'l Conf. on Welding Low Temp. Containment Plant, Welding Institute, London, England, Paper 3, (November 1973), p. 251.
5. H. Fredrics, C. Nap, H. van der Winden: Met. Constr., 9, (3) and (4), 104-107, 162-165, (March 1977).
6. K. W. Mahin, J. W. Morris, Jr., and I. Watanabe: "A Review of the Development of Ferritic Consumables for the Welding of 9% Nickel Steel: Research in the U.S. and Japan". Presented at the 1979 Int'l Cryogenic Mat'ls. Conf., Madison, Wisconsin, (August 20-24, 1979).
7. I. Watanabe: Autumn Meeting of the Japan Welding Engineering Society, (September 1977).
8. F. H. Lang: "Ferritic Steel Welding Material". United States Patent 3,218,432 (November 1965).

Table 1: Amco Steel's A553 Grade A Plate

CHEMICAL COMPOSITION:

FE	NI	C	MN	SI	P	S	H	O	N
Bal.	9.18	.068	.49	.22	.012	.010	2ppm	10ppm	10ppm

MECHANICAL PROPERTIES:

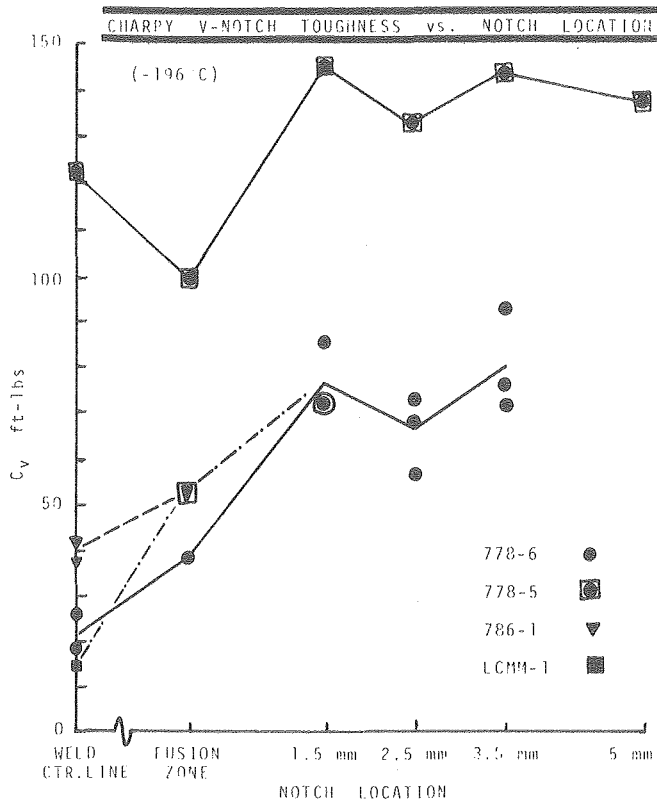
ORIENTATION & TEMPERATURE		Y.S. ksi (MPa)	T.S. ksi (MPa)	ELONG. (%)	R.A. (%)	C _v ft-lb (J)
25°C	L	102 (703)	113 (779)	29	73	115 (156)
	T	102 (703)	112 (772)	28	71	66 (90)
-196°C	L	137 (945)	170 (1172)	29	66	69 (94)
	T	136 (938)	169 (1165)	29	58	41 (56)

Table 2: Chemical Compositions of the Ferritic Gas Shielded Arc Wires (L.B.L.)

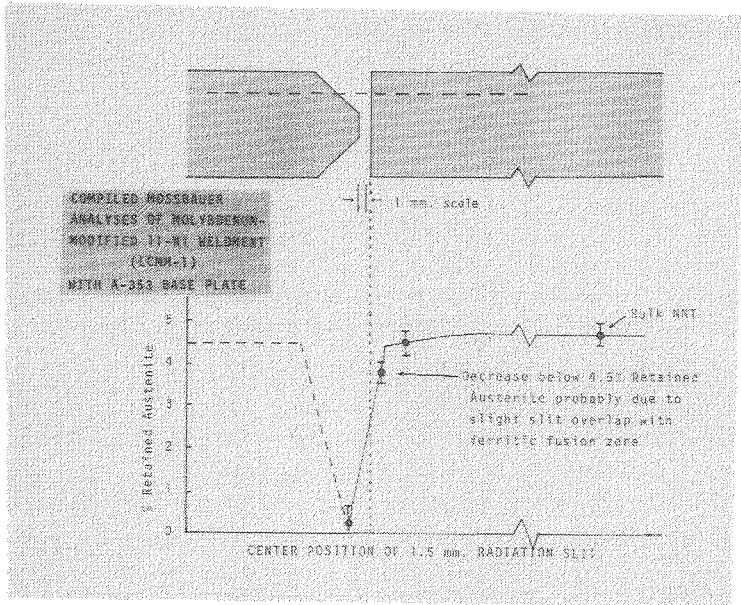
ALLOY	Fe	Ni	C	Mn	Mo	Si	Ti	Al	O
778-5	Bal.	11.06	.023	.22	----	----	----	----	40ppm
778-6	Bal.	10.98	.056	.20	----	.14	.05	.04	130ppm
Mo-Mod.* 11Ni	Bal.	11.5	.054	.24	.33	----	.07	.02	10ppm
LCMM-1	Bal.	12.25	.02	.34	.32	----	.03	.04	20ppm

* Nitrogen Level after Swaging: 100ppm
 Hydrogen Level " " : 30ppm

Fig. 1: Weldment Impact Toughnesses Obtained for the Four Ferritic Gas Metal Arc Weld Wires

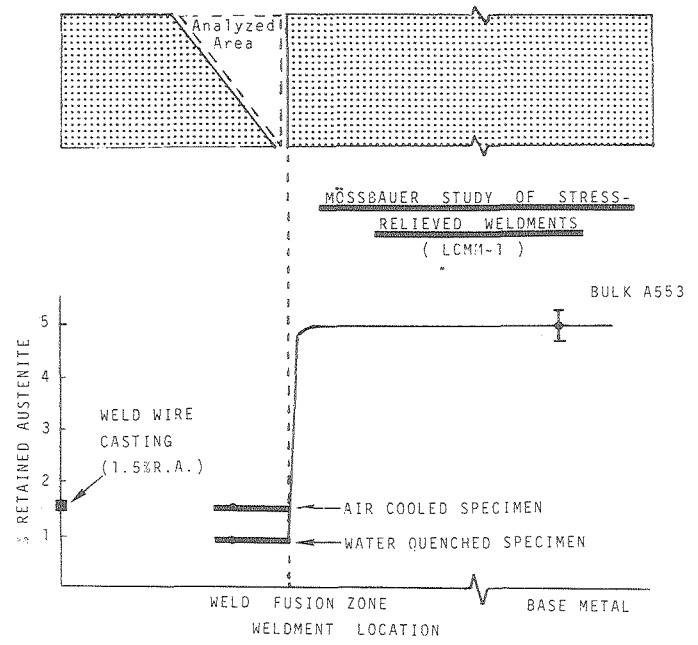


XBL 798-11022



CBB798 10508

(a) As-Welded Sample: No Retained Austenite in Weld Deposit



(b) Stress-Relieved Sample and Casting of Similar Composition to Weld Deposit

Fig. 2: Mössbauer Scans of Weldment LCMM-1

WELD MICROSTRUCTURE vs. FRACTURE MODE (-196°C)

(Low Carbon, Mo-Modified 12Ni Filler)

$C_v = 25 \text{ ft-lb (34J)}$

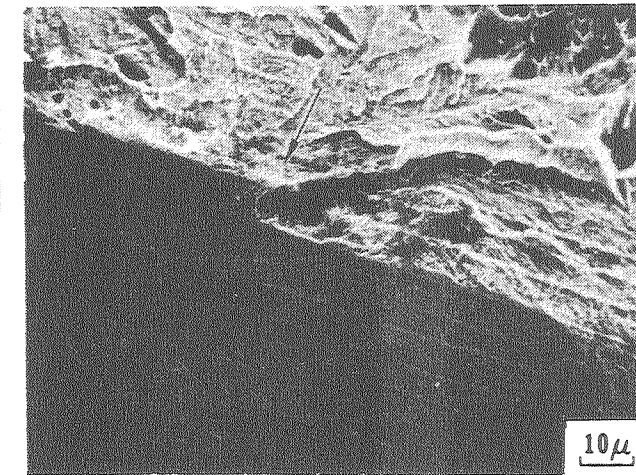
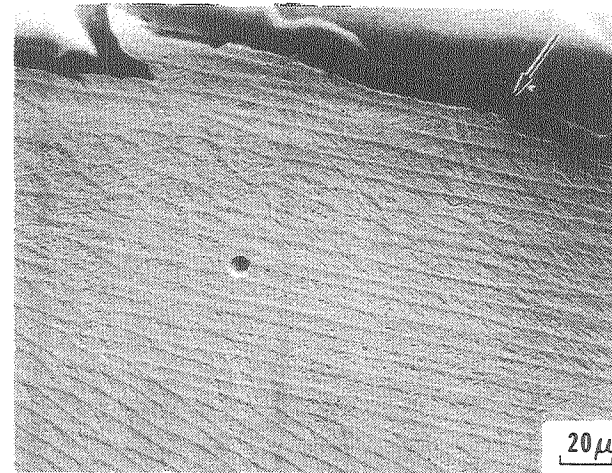
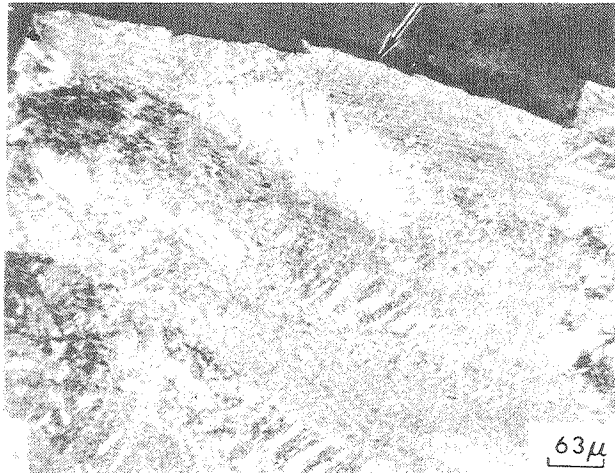
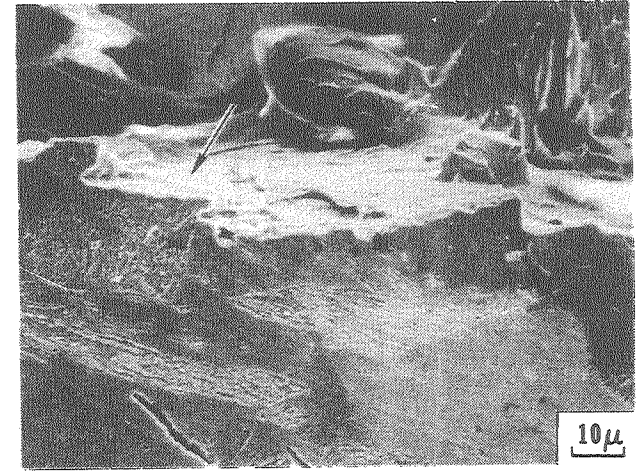
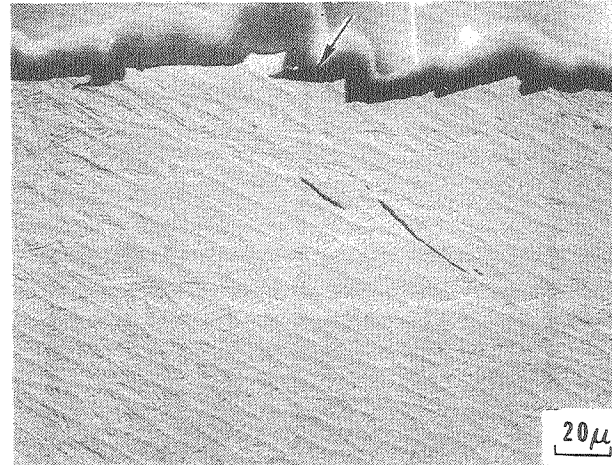
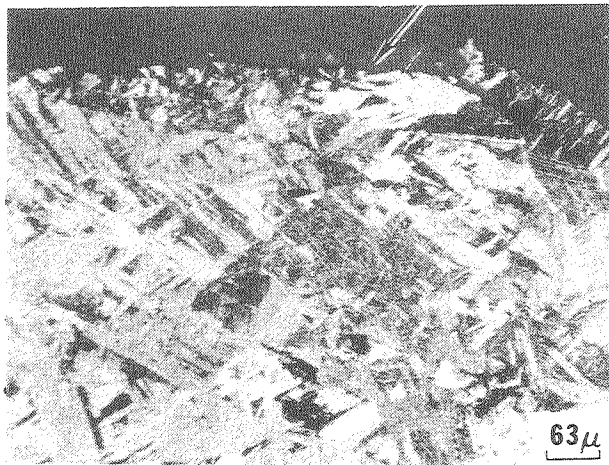


Figure 3. Optical and Scanning Electron Micrographs of the LC11-1 Weld Microstructure vs. Fracture Mode

XBB 798 10357

FRACTURE MODE vs. WELD MICROSTRUCTURE (-196°C)
(Mo - Modified 11-Ni Filler Wire)

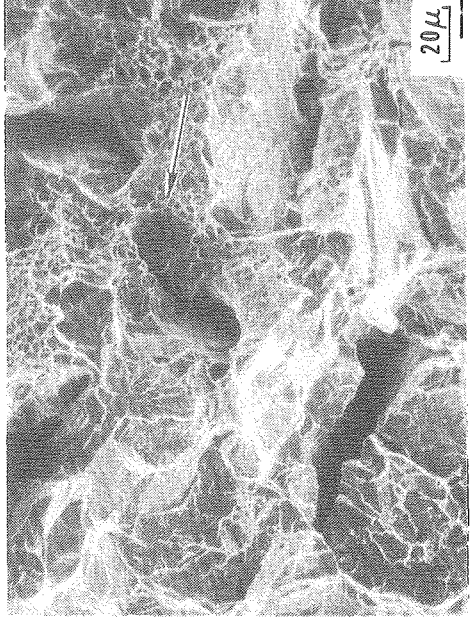
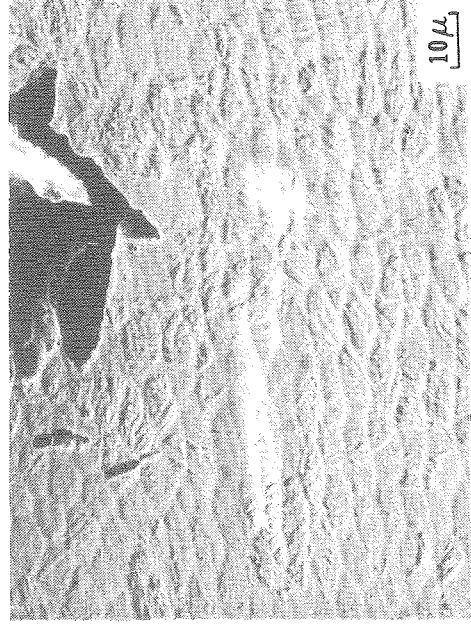
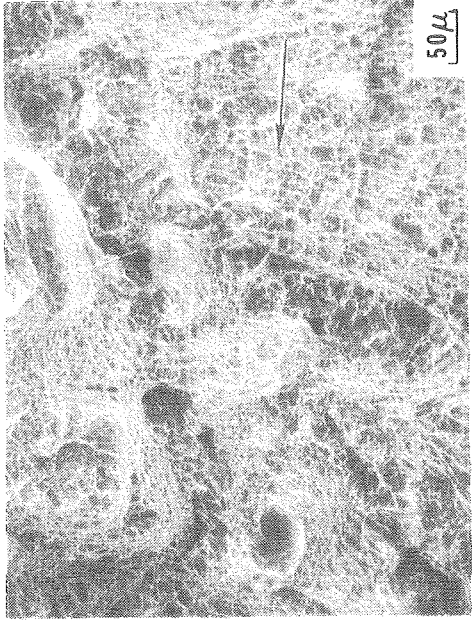
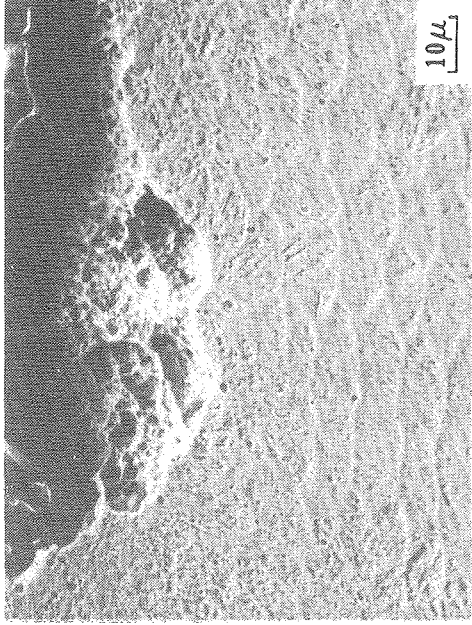
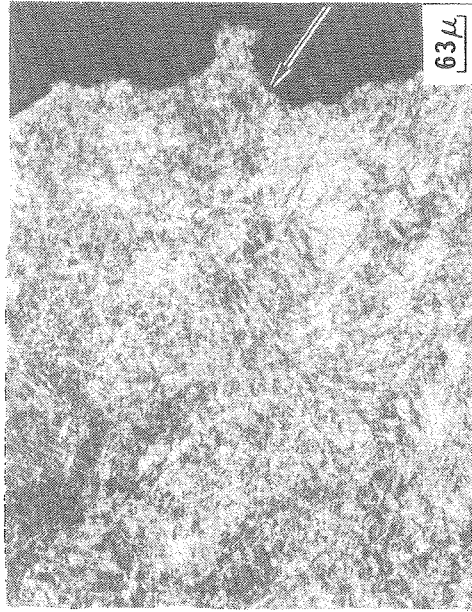
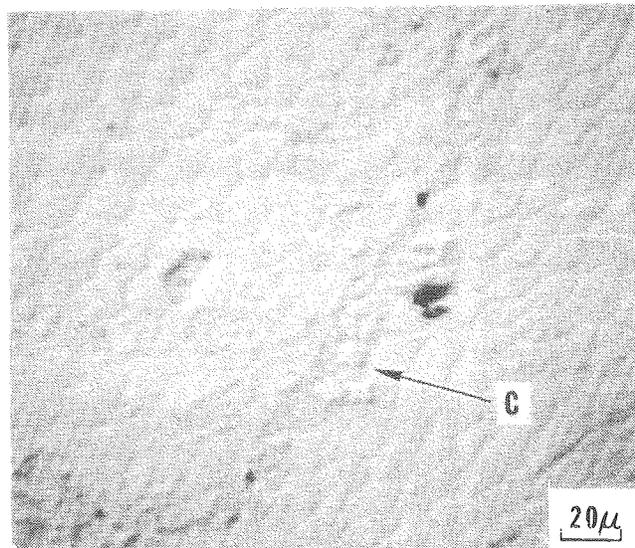


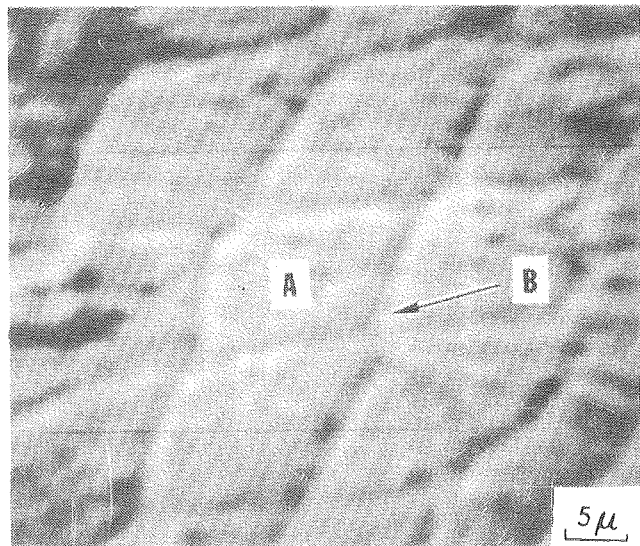
Figure 4

XBB 798 10353

AUGER SPECTRUM FOR POLISHED WELD METAL SURFACE



$E_p = 5 \text{ kv}$



Specimen: LCMM - 1

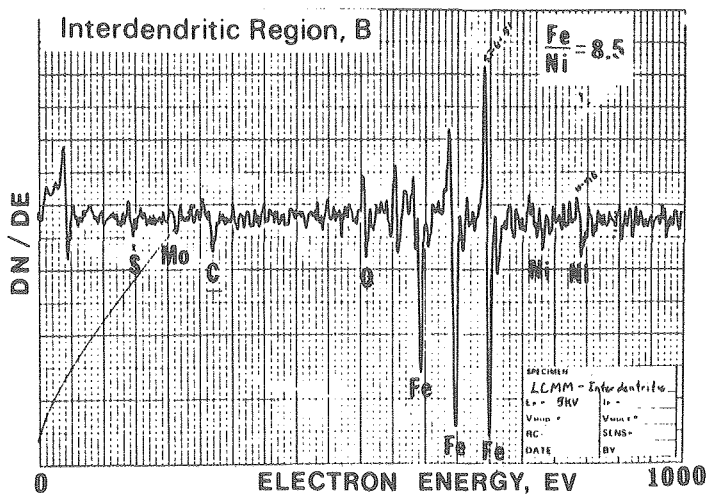
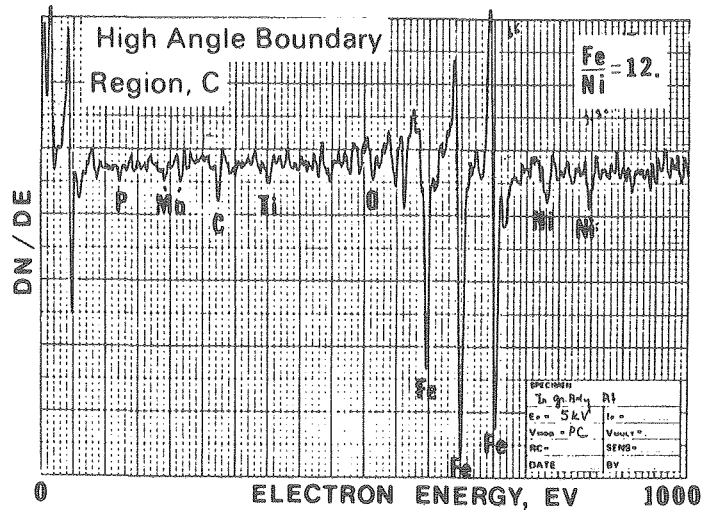
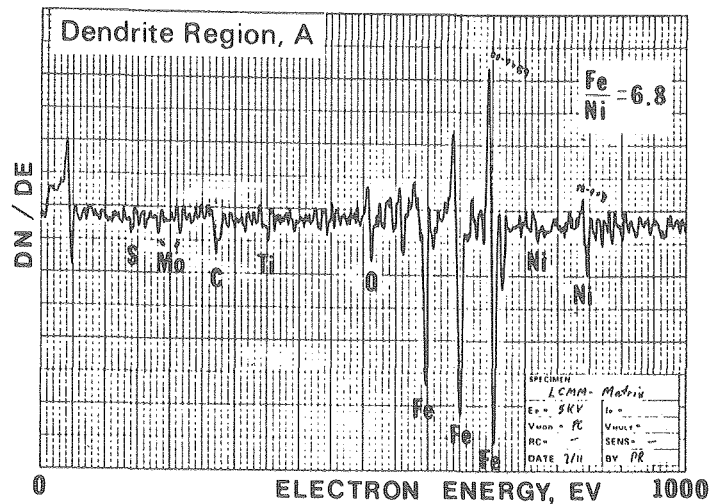
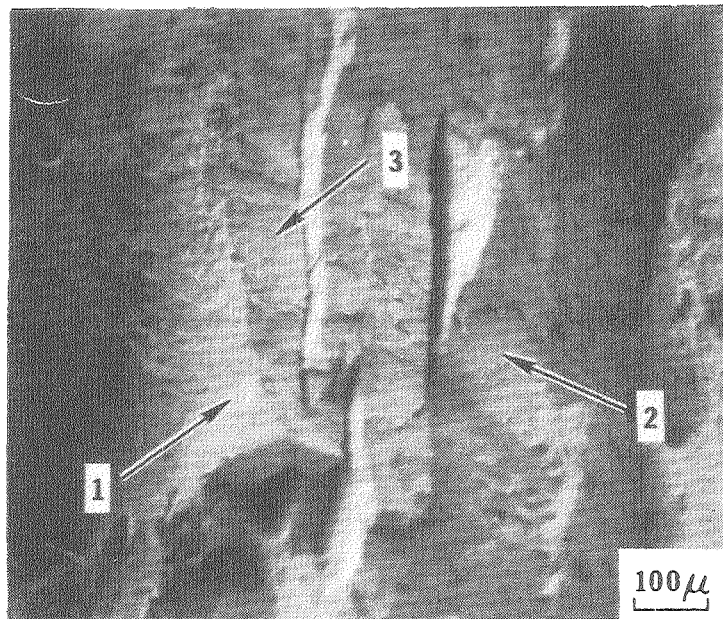


Figure 5.

AUGER SPECTRUM FOR CVN FRACTURE SURFACE



Specimen: LCMM-1

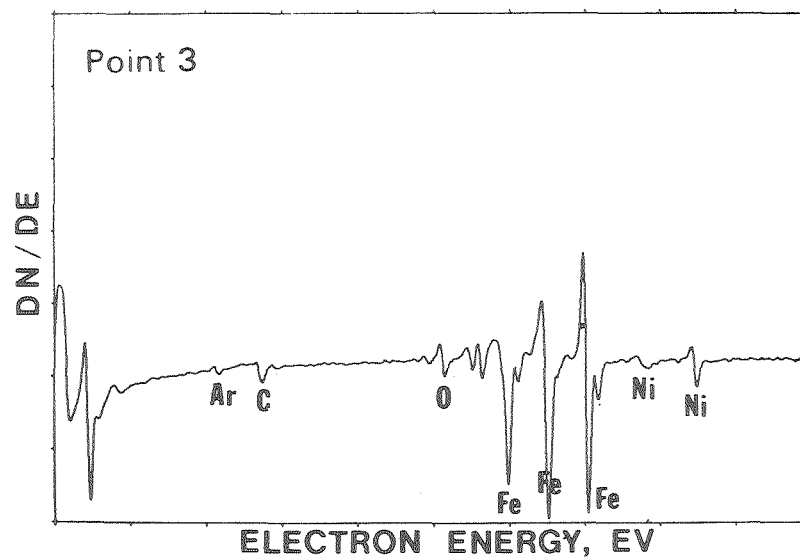
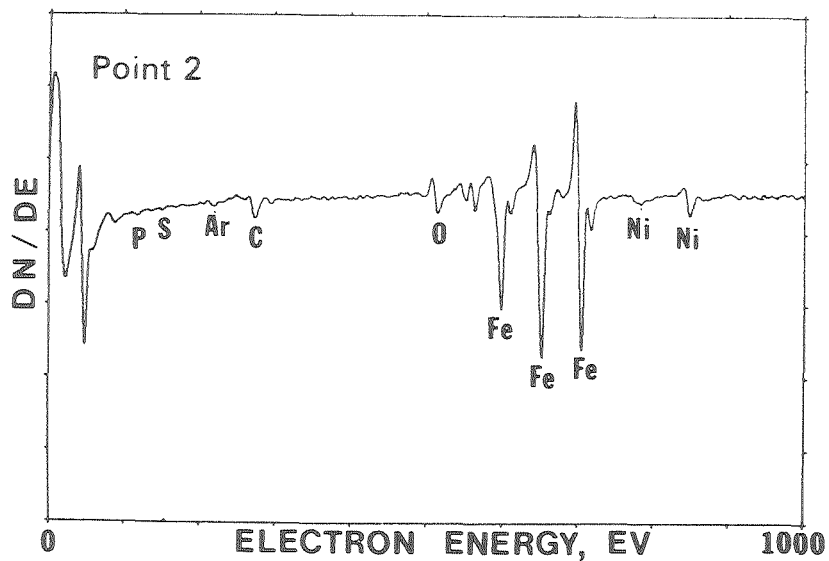
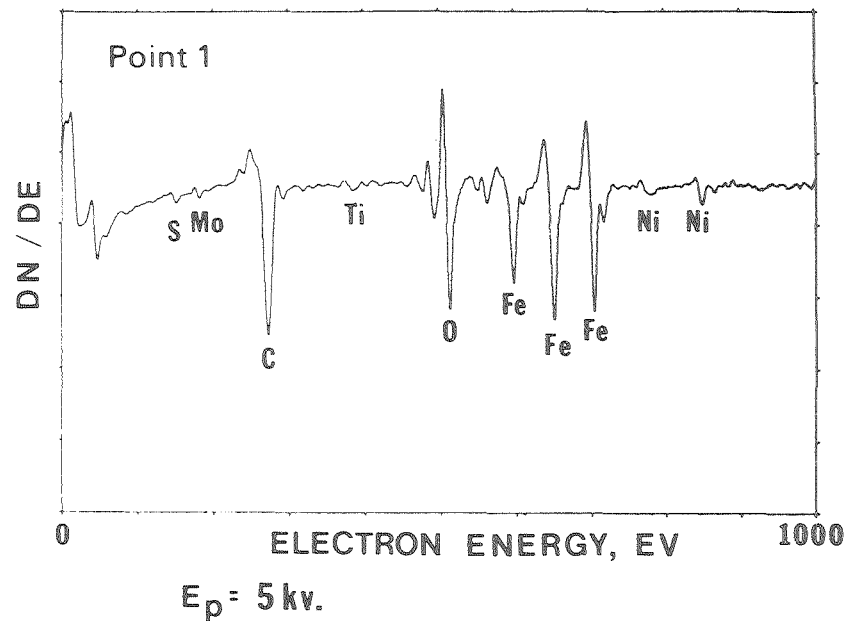


Figure 6.

XBB 798 10354